fishes

MDPI

Article

Impact of Exposure Routes of Copper Oxide Nanoparticles in the Clam *Ruditapes decussatus*

Maria J. Bebianno [1,*], Mustafa Tuncsoy [1,2], Thiago L. Rocha [1,3], Tania Gomes [1,4] and Taina Garcia [1]

[1] CIMA/ARNET, Centre for Marine and Environmental Research/Aquatic Research Network, University of Algarve, Campus de Gambelas, 8000-139 Faro, Portugal; mustafa_tuncsoy@hotmail.com (M.T.); thiagorochabio20@ufg.br (T.L.R.); tania.gomes@niva.no (T.G.); taina-garcia@hotmail.com (T.G.)
[2] Faculty of Science and Letters, Biology Department, University of Cukurova, Sarıçam 01250, Adana, Turkey
[3] Laboratory of Environmental Biotechnology and Ecotoxicology, Institute of Tropical Pathology and Public Health, Federal University of Goiás, Goiânia 74605-050, Brazil
[4] Norwegian Institute for Water Research (NIVA), Økernveien 94, 0579 Oslo, Norway
* Correspondence: mbebian@ualg.pt

Abstract

The increasing production of diverse applications of engineered nanoparticles along with their potential release into the marine environment from both point and diffuse sources have become a significant concern for ocean health. Due to their unique physical properties, particularly their high surface-to-volume ratio, these nanoparticles can exhibit enhanced bioavailability and toxicity to marine biota. Copper oxide nanoparticles (CuO NPs) are especially prevalent due to their wide range of commercial applications. In the aquatic environment, these nanoparticles typically become part of colloidal fraction and are subjected to physicochemical transformations, leading to the formation of aggregates that eventually sink and deposit onto the bottom substrate. Therefore, sediments, in addition to the water column, act as the primary route of exposure to benthic organisms. The clam *Rudipates decussatus* is a marine suspension-feeder of great ecological and economic importance in Europe. *Ruditapes decussatus* were exposed to CuO NPs (10 μg L^{-1}) or an equivalent concentration of ionic copper (Cu^{2+}) in both water and water/sediments matrices for 15 days to compare the toxicological impact of different exposure routes. Copper accumulation was monitored in both gills and digestive gland, alongside various biomarkers of susceptibility, exposure, and damage. The results revealed distinct uptake patterns that were dependent on the exposure routes, the chemical form of the metal and the specific tissue responses. Highlighting the complex impact of these contaminants on marine biodiversity.

Keywords: nanoparticles; biomarkers; oxidative stress; genotoxicity; neurotoxicity

Key Contribution: Impact of routes of uptake of copper nanoparticles on *Ruditapes decussatus*.

Academic Editor: Youji Wang

Received: 31 March 2026
Revised: 30 April 2026
Accepted: 6 May 2026
Published: 9 May 2026

1. Introduction

The increasing production of engineered nanoparticles (ENPs) (particles with at least one dimension between 1 and 100 nm), of various types and applications in everyday life, along with their potential release into the ocean from point and diffuse sources and their subsequent effects on marine species at the various levels of biological organization, ocean health, and human health, has become a cause for concern [1] and needs to be assessed within the context of the One Health approach [2]. Through an integrated, systems-based framework that recognizes the interdependence of human, animal, and environmental

health, the One Health approach seeks to enhance population well-being, strengthen disease prevention and control, and ensure ecosystem resilience and long-term sustainability [3].

Among ENPs, metallic nanoparticles are particularly relevant due to their extensive industrial and commercial applications [4]. Copper oxide nanoparticles (CuO NPs), for example, are widely used for their antimicrobial properties and high thermal and electrical conductivity [5]. In contrast, ionic copper is naturally abundant, commonly present in mineral salts and organic compounds, and widely used in antifouling paints, while also playing essential biological roles [6,7]. Despite their importance, ENPs remain emerging contaminants, with limited detection methods in aquatic systems and a lack of robust environmental risk assessment strategies [8].

The behavior and toxicity of metallic ENPs differ from their ionic counterparts. Due to their high surface area-to-volume ratio, ENPs can interact with biological membranes, penetrate cells, and generate reactive oxygen species (ROS), driven by both particle reactivity and ion release [9,10]. However, the low dissolution of CuO NPs in seawater suggests that their toxic effects may largely arise from nanoparticle-specific properties rather than solely from released ions [11,12]. Indeed, CuO NPs have been reported to be more toxic than ionic copper under certain conditions [13,14].

Once in seawater, ENPs can aggregate, undergo physicochemical transformations, and settle into sediments, where they may accumulate or later resuspended into the water column [15]. This dynamic behavior increases exposure risks for benthic and suspension-feeding organisms, which can ingest particles from sediments, pore water, or the sediment–water interface [16]. Given the ecological importance of benthic environments and their role in food webs, understanding the fate and effects of ENPs in sediments remains challenging. Therefore, ecotoxicological approaches using biochemical biomarkers as early warning indicators are essential for assessing nanoparticle impacts [17].

Marine bivalves are particularly suitable for such assessments due to their filter-feeding behavior and capacity to accumulate contaminants. The grooved carpet shell clam, *Ruditapes decussatus*, is widely used as a bioindicator species and is also of commercial importance [18]. Exposure to nanoparticles can induce oxidative stress, protein damage, and genotoxic effects in marine organisms [19,20]. However, responses to CuO NPs and ionic copper vary across species and exposure pathways. For instance, sediment-bound CuO NPs have been shown to increase mortality in amphipods, while aqueous exposure to ionic copper may have stronger effects in polychaetes [16,21,22]. Differences in bioaccumulation patterns between nanoparticles and dissolved copper further suggest distinct uptake routes among species [11].

In this context, the present study aims to compare the accumulation and toxic effects of CuO NPs and dissolved copper in *Ruditapes decussatus* under different exposure scenarios. A comparative approach was applied using water-only and combined water–sediment systems contaminated via the water column, to assess the influence of exposure matrices on toxicity. Environmentally relevant concentrations were selected based on labile copper levels reported in seawater [12,23]. A suite of biomarkers was used to evaluate biological responses, including antioxidant defenses (SOD, CAT, GST), metallothionein induction (MT), oxidative damage (LPO), neurotoxicity (AChE activity), and genotoxicity (comet assay). These responses were measured in gills, digestive glands, and the hemolymph key target tissues for contaminant uptake. This integrated approach supports the evaluation of copper toxicity within a One Health perspective.

2. Materials and Methods

2.1. CuO NP Characterization

Copper (II) oxide nanoparticles (CuO NPs) were purchased from Sigma-Aldrich (St. Louis, MO, USA), with a manufacturer-specified size of <50 nm. A CuO NP stock solution (10 mg Cu L^{-1}) was prepared by dispersing the nanoparticles in Milli-Q water, followed by sonication for 15 min using a bath-type sonicator (Ultrasonic bath, VWR International, Oeiras, Portugal; 230 V, 200 W, 45 kHz). The suspension was kept under constant stirring throughout the 15-day experiment to maintain the nanoparticles in suspension [19]. A copper sulfate (Cu^{2+}) stock solution was prepared in a similar manner but without sonication.

The size distribution of 250 randomly selected nanoparticles was determined in natural seawater by transmission electron microscopy (TEM) (JEM-1230 (JEOL, Tokyo, Japan). CuO NPs (100 mg L^{-1}) were diluted in ultrapure water, sonicated, and a drop of the suspension was placed on a Ni grid and allowed to dry before examination at 80 kV. The mean size of particles and agglomerates/aggregates in natural seawater was further characterized over a 12-h period (corresponding to the interval between water renewal and CuO NP re-dosing) using dynamic light scattering (DLS) with an ALV apparatus equipped with an Ar ion laser (ALV GmbH, Langen, Germany) (515.5 nm), following [19]. Images were acquired using a JEM-1230 (JEOL, Japan) TEM coupled to a digital camera (Gatan model 785 ES1000W Erlang Shen CCD, London, UK).

Zeta potential, also determined by DLS, provides information on the surface charge of nanoparticles in colloidal suspensions, reflecting the attraction of a thin layer of oppositely charged ions to the nanoparticle surface. It is commonly used to estimate colloidal stability [24], with values greater than +25 mV or less than −25 mV generally indicating high stability [25].

2.2. Experimental Design

Clams (*R. decussatus*) were obtained from an aquaculture farm in the Ria Formosa lagoon (Portugal) (37°1′28.92″ N; 7°50′39.20″ W), transported alive to the laboratory, and acclimated for 7 days under constant aeration and controlled temperature (18 ± 2 °C).

Sediments used in the bioassays were also collected from the Ria Formosa at a depth of 30 m using a core sampler, in collaboration with the SIHER Project (Processes of Sedimentary Infilling and Holocene Evolution of the Ria Formosa Lagoon System) at CIMA, University of Algarve. This procedure ensured that reference sediment samples were minimally affected by anthropogenic influence. After collection, sediments were continuously aerated for 10 days to stabilize their pH (7.8 ± 0.2). Due to their fine grain size and muddy composition, which could interfere with normal feeding and respiration by clogging the bivalves' siphons, a clean, washed sand fraction collected from Faro Beach (southern Portugal) was added to adjust sediment grain size distribution. This approach is consistent with standard sediment toxicity testing guidelines for formulated sediments, allowing the survival, growth, or reproduction of a variety of benthic invertebrates [26,27]. Thus, the sediments used in the experiments consisted of 34% silt and clay (<0.062 mm) and 66% sand (0.25–0.5 mm), based on grain size distribution.

After the acclimation period, two experimental systems were established in a triplicate design: (i) a water system containing 5 L of natural seawater (from the Ria Formosa lagoon), and (ii) a water–sediment system containing 4 L of natural seawater and 1 L of reference sediments. For both systems, three experimental treatments were tested: control (CT), CuO nanoparticles (CuNP), and $CuSO_4$ (Cu). Twenty clams (2.5 clams L^{-1}) were placed in polyethylene aquaria in a triplicate design. Individuals were exposed via the water column to the same nominal Cu concentration (10 µg Cu L^{-1}), either in nanoparticulate form (CuO

NPs) or as its dissolved counterpart ($CuSO_4$). The selected Cu concentration was based on realistic global environmental levels reported for marine and coastal ecosystems [12,23].

To prevent nanoparticle aggregation/agglomeration, water was renewed every 48 h, and Cu concentrations were re-established by direct pipetting into the water column. Water renewal was performed carefully to avoid disturbing nanoparticle stability and sediment resuspension, and to minimize additional stress to the organisms. Animals were fed exclusively through the natural seawater renewed throughout the experiment. Over the 15-day bioassay, systems were maintained under constant aeration and a controlled photo period. Physicochemical parameters (temperature 17 ± 2 °C, salinity 34, pH 7.5 ± 0.4) were measured daily using a multiparameter probe (YSI 556MPS, YSI, Yellow Springs, OH, USA).

Clams were sampled from the experimental setup on day 0, day 7, and day 15 of exposure for biochemical and genotoxic analyses. Clams were weighed and measured. For DNA damage assessment, hemolymph was immediately extracted from the posterior adductor muscle (n = 6 clams per treatment) using a sterile hypodermic syringe and kept on ice for immediate analysis. Gills and digestive glands (n = 6 clams per treatment) were individually dissected, frozen in liquid nitrogen, and stored at −80 °C for subsequent homogenization and biomarker analyses. These included oxidative stress biomarkers (superoxide dismutase—SOD; catalase—CAT), biotransformation activity (glutathione S-transferases—GSTs), metallothioneins (MTs), cell membrane damage (lipid peroxidation—LPO), and neurotoxicity (acetylcholinesterase activity—AChE).

2.3. Condition Index (CI)

To assess the physiological status of the bivalves (n = 9 clams per treatment) from each treatment were individually weighed using the ratio: Condition index (CI) = (drained weight (g) and dry shell weight [28].

2.4. Metal Analysis

The gills and digestive gland (3 replicates for each condition, pools of 2 gills/digestive gland), were wet digested with HNO_3 (80 °C) and Cu concentration was determined by atomic absorption spectrophotometry. Digested samples were then applied to graphite furnace atomic absorption spectrometry (AAS AAnalyst 800, Perkin-Elmer, Rodgau, Portugal).

For quality control assurance, a standard reference material (Lobster Hepatopancreas—TORT II.) from the National Research Council (Canada) was used, with Cu levels of the samples (106.4 ± 2.4 μg Cu kg^{-1} d.w.) with similar levels of those of the reference material (106 ± 10 μg Cu kg^{-1} d.w.).

2.5. Total Protein Content

Total protein concentration (mg protein g^{-1} tissue) was determined in gills and digestive glands according to the method described by Bradford [29], using Bovine Serum Albumin as a standard.

2.6. Antioxidant Enzymes

Clam gills and digestive glands (n = 6) were homogenized in 5 mL of ice-cold 20 mM Tris–sucrose buffer (0.5 M sucrose, 0.075 M KCl, 1 mM DTT, 1 mM EDTA, pH 7.6). The homogenization was performed using a VWR Star-Beater (VWR International, Portugal) for 5 min at 20 shakes s^{-1} with grinding beads. The cytosolic fraction was subsequently obtained through a two-step centrifugation process: first at 1500× *g* for 15 min at 4 °C, followed by a second centrifugation at 12,000× *g* for 45 min at 4 °C. Aliquots of the resulting supernatant were then used to determine the activities of the antioxidant enzymes (SOD and CAT), as well as the biotransformation enzyme GST.

The activity of SOD was quantified, in the cytosolic fraction, by the variation in absorbance (at 550 nm) in cytochrome c oxidase reduction to cytochrome c reductase, triggered by xanthine oxidase/hypoxanthine system [30]. SOD activity is expressed in terms of mmol min^{-1} mg $protein^{-1}$. Catalase enzymatic activity was measured spectrophotometrically by the absorbance decrease at 240 nm, owing to hydrogen peroxide (H_2O_2) consumption [31] and is expressed in µmol min^{-1} mg $protein^{-1}$. Glutathione S-transferases activity was estimated by the change in the absorbance of the reaction conjugate which consisted of reduced glutathione (GSH) with 1-chloro-2,4-dinitrobenzene (CDNB), in a buffer solution of KH_2PO_4/K_2HPO_4, by the adapted method of Habig et al. (1974) [32]. GST activity is expressed in µmol min^{-1} mg $protein^{-1}$.

2.7. Metallothioneins

Gills and digestive glands of *R. decussatus* (n = 6) were homogenized in Tris-HCl buffer (0.02 M, pH 8.6) and butylated hydroxytoluene (BHT) (10 µL BHT per mL Tris–HCl buffer). The homogenate was centrifuged at 30,000× *g* for 45 min (4 °C). Aliquots of the supernatant were separated for LPO and total protein quantification. The remaining supernatant was heat-treated at 80 °C for 10 min to precipitate the high-molecular-weight proteins, and re-centrifuged at 30,000× *g* for 45 min at 4 °C. The obtained cytosolic fraction was stored at −80 °C for the following MT quantification by differential pulse polarography. Quantification of MT was determined by differential pulse polarography using a Eco Chemie µAutolab III potentiostat, Metrohm 663VA stand, Portugal according to the method described by Bebianno and Langston [33].

2.8. DNA Damage

Single cells with DNA damage were detected by the Comet assay, according to the method proposed by Singh et al. [34] and adapted by Gomes et al. [35]. Extracted haemolymph (150 µL) was individually centrifuged at 3000 rpm for 3 min (4 °C). The obtained cell pellets were suspended in 0.65% low melting point agarose (LMA, in Kenny's salt solution) and spread onto the microscope slides coated with 0.65% normal melting point agarose (NMA) in Tris-EDTA. Slides were then immersed in lysis buffer (2.5 M NaCl, 100 mM EDTA, 10 mM Tris, 1% Triton X-100, 10% dimethyl sulfoxide, 1% Sarcosil, pH 10, 4 °C) for 1 h, to disrupt cellular membranes, remove soluble cellular components and immobilize DNA in agarose.

Subsequently, slides were placed in an electrophoresis chamber containing alkaline buffer (300 mM NaOH, 1 mM EDTA, pH 13, 4 °C) and left for 15 min to allow DNA unwinding and the expression of strand breaks. Electrophoresis was carried out for 5 min at 25 V and 300 mA. Slides were stained with 4,6-diamidino-2-phenylindole (DAPI, 1 $mgmL^{-1}$) and the presence of the produced tails analysed using an optical fluorescence microscope (Zeiss Axiovert S100, Jena, Germany) coupled with a camera (Sony, Lisbon, Portugal). DNA damage was quantified using Komet 5.5 image analysis software (Kinetic Imaging Ltd., Nottingham, UK) by scoring 50 randomly selected cells per slide (25 per gel per individual) at ×400 magnification.

2.9. Acetylcholinesterase Activity (AChE)

Acetylcholinesterase (AChE) activity was determined in the gills (n = 6) according to the method described by Ellman et al. [36] using the increased 5-mercapto-2-nitrobenzoate formation following the absorbance of the reaction with thiocholine (substrate) and DTNB at 412 nm (ε = 13.6 mM^{-1} cm^{-1}). The AChE activity is expressed in nmol min^{-1} mg $protein^{-1}$.

The increase in 5-mercapto-2-nitrobenzoate, a compound of yellow color produced due to the non-enzymatic reaction of thiocholine with 5,5′-dithio-bis (2-nitrobenzoic acid),

was used to determine the acetylthiocholine degradation rate. Absorbance was read at 412 nm and results expressed in nmol ACTC min^{-1} mg of total protein concentration.

2.10. Lipid Peroxidation (LPO)

Gills and digestive gland of clams from each condition (n = 6) were homogenized individually in 100 mM Tris–HCl buffer (pH 8.6) and 100:1 µL of Triton, on ice, using a VWR Star-Beater (5 min, 20/s shaking, with grinding balls) and then centrifuged at 12,000× *g* for 30 min (4 °C). Supernatants were separated into aliquots for total protein determination and LPO levels. LPO levels were quantified following a method adapted from Erdelmeier et al. [37]. The assay was based on the spectrophotometric detection of malondialdehyde (MDA) and (2E)-4-hydroxy-2-nonenal (HNE), with absorbance measured at 540 nm. LPO values were expressed as nmol of MDA equivalents per mg of protein (nmol mg^{-1} protein).

2.11. Statistical Analysis

All statistical analyses were performed using Statistica 8.0 software (StatSoft Inc., Tulsa, OK, USA). Data from genotoxicity (Comet assay) and biochemical biomarkers (SOD, CAT, AChE, GST and LPO) were tested for normality (Shapiro–Wilk test) and homogeneity of variances (Levene's test). Once assumptions of normality and homoscedasticity were met, differences among treatments were assessed using one-way analysis of variance (ANOVA), followed by Tukey's post hoc multiple comparison test, or the non-parametric equivalent test (Kruskal–Wallis), when assumptions were not met. The influence of the time of exposure (0, 7 and 15 days), copper form treatment (control, Cu-ionic, and CuO-NPs) and their interactive effects were analysed through a two-way analysis ANOVA (see Supplementary Material, Table S1). Comparisons were conducted separately for each tissue and exposure matrix. Within each condition, treatments were compared across exposure times (e.g., CT7 vs. CT15), and differences among treatments were also evaluated within each time point (e.g., CT7 vs. CuNP7). Additionally, comparisons between exposure matrices (water vs. sediment) were conducted for the same tissue and treatment conditions, to assess differences between exposure scenarios. Statistical significance was considered at $p < 0.05$.

A multivariate Principal Component Analysis (PCA) was applied to integrate all variables (biomarkers), exposure matrices, tissues, time points, and treatments. PCA was used to explore patterns of variation and identify correlations between biomarkers and experimental conditions. A hierarchical cluster analysis was performed using a Euclidean distance matrix to assess similarities among treatments based on biomarker responses. Clustering was conducted using the unweighted pair-group method with arithmetic mean (UPGMA), and results were represented as a dendrogram, where the distance between clusters reflects the degree of dissimilarity among samples.

3. Results and Discussion

3.1. CuO NPs Characterization

Understanding the physicochemical characteristics and behavior of CuO NPs in aquatic media is essential to assess their bioavailability and potential toxicity. Particle size and distribution are presented in Table 1. Primary particle size, determined by transmission electron microscopy (TEM) in natural seawater, showed a median diameter of 38.2 ± 1.4 nm Figure 1, slightly differing from the manufacturer's specification.

Table 1. Characterization of CuO NPs by Transmission Electron Microscope (TEM) and Dynamic Light Scattering (DLS). Values are the mean ± std.

Particle Characteristic	Method	CuNP
Size (nm)	TEM	<50 [a]
Particle size distribution (nm)	TEM	38.2 ± 1.4 [b]
Mean diameter (nm)	DLS	258.7 ± 4.7 [b]
Zeta potential (Mv)	DLS	−26.3 ± 0.3 [b]

[a] Information from manufacturer Sigma-Aldrich. [b] 100 mg. CuNP/L in Milli-Q water.

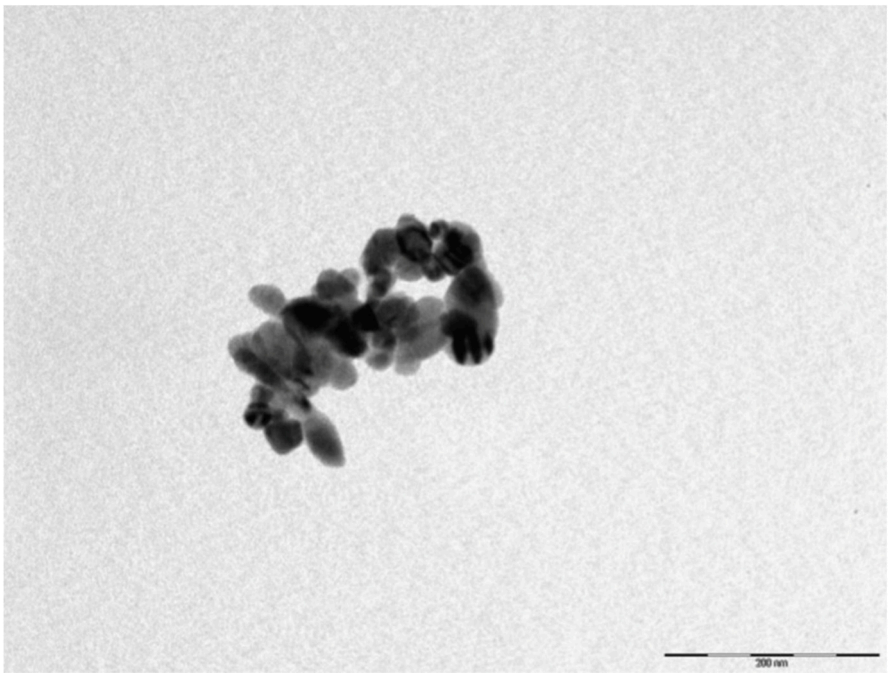

Figure 1. Transmission electron microscopic image of CuO nanoparticles at 100 mg L^{-1} in ultrapure water.

Gomes et al. [19] reported that ~53% of CuO NPs (10 µg L^{-1}) were removed from the water column within 12 h, mainly due to sedimentation, while copper dissolution remained below 1%, indicating that most copper persisted in nanoparticle form. Similarly, CuO NPs (25–55 nm) produced by different synthesis methods exhibited aggregation and polydispersity, with limited, synthesis-dependent dissolution [38].

Aggregation appears to be a general behavior of CuO NPs in seawater. Even surface-modified CuO NPs (10–20 nm), including neutral (PEG), negatively charged (COOH), and positively charged (amine, NH_3) coatings, formed large aggregates (1137–1530 nm) with similar size distributions, regardless of surface functionalization [39].

3.2. Condition Index (CI)

To ensure that observed effects were not confounded by organism condition, the condition index (CI) of *Ruditapes decussatus* was monitored (Table 2). CI remained stable in most treatments, indicating that clams were maintained in good physiological condition throughout the experiment. A significant decrease was observed only in clams exposed to ionic copper in the water system, from 0.26 ± 0.02 to 0.23 ± 0.02 after 15 days ($p < 0.05$). No significant temporal or treatment-related differences were detected in clams exposed to CuO NPs or in either water/sediment system ($p > 0.05$), confirming comparable physiological status across treatments.

Table 2. Condition index of the clams *Ruditapes decussatus* unexposed and exposed to CuO NPS and $CuSO_4$ in water and in water/sediments systems.

	Exposure System	Time of Exposure (Days)		
		0	7	15
Control	water	0.25 ± 0.02	0.26 ± 0.03	0.26 ± 0.02
	water/sed	0.26 ± 0.02	0.26 ± 0.05	0.25 ± 0.02
CuO NPs	water		0.26 ± 0.03	0.25 ± 0.02
	water/sed		0.25 ± 0.03	0.26 ± 0.03
$CuSO_4$	water		0.27 ± 0.02	0.23 ± 0.02
	water/sed		0.25 ± 0.03	0.25 ± 0.05

3.3. Copper Accumulation

Copper is an essential metal involved in enzymatic processes and MTs, but elevated concentrations can be toxic, particularly to bivalves. No significant changes in copper levels were observed in control clams ($p > 0.05$; Figure 2). In exposed clams, copper accumulation was tissue, copper form, and exposure matrix dependent, with higher concentrations consistently observed in the digestive gland.

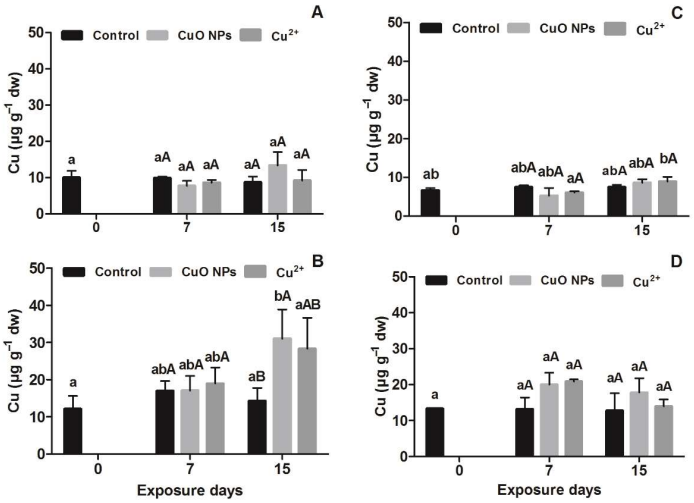

Figure 2. Copper concentrations (µg g^{-1} dry weight) detected in gills and digestive gland of *R. decussatus* unexposed or exposed to CuO NPs and to Cu^{2+} for 15 days in water (**A**,**B**) and in a water/sediment matrix (**C**,**D**). Capital letters represent differences between treatments at the same time of exposure and lower letters differences between time of exposure ($p < 0.05$).

Gills, as the primary interface with the environment, showed limited accumulation. In the water system, copper levels increased slightly under CuO NP exposure but not significantly ($p > 0.05$) and remained unchanged under ionic copper. No differences were detected between copper forms (Figure 2A). In the water/sediment system, gill copper levels were lower and similar across treatments, indicating reduced bioavailability compared to the water-only system (Figure 2C).

In contrast, the digestive gland showed significant accumulation. In the water system, copper levels increased over time, reaching 1.8-fold (CuO NPs) and 1.4-fold (ionic copper) higher than initial levels ($p < 0.05$; Figure 2B). No such increase was observed in the water/sediment system ($p > 0.05$; Figure 2D). These results suggest that CuO NPs taken up at the gills may be processed and transferred to the digestive gland, the main site of accumulation and detoxification.

Nanoparticle uptake in bivalves likely occurs via endocytosis, particularly for particles incorporated into aggregates, although translocation depends on particle size and aggregation state [12,40]. Differences between species further highlight distinct uptake pathways. For example, higher accumulation of ionic copper than CuO NPs has been reported in freshwater mussels, whereas the opposite trend was observed in polychaetes [11,41]. In *R. decussatus*, copper accumulation in the digestive gland follows first-order kinetics with a half-life of 10–12 days [42], indicating active regulation and detoxification.

Given that copper can promote ROS generation via Fenton-type reactions, it is essential to evaluate whether CuO NPs induce similar oxidative responses.

3.4. Antioxidant Enzymes

Although the mechanisms underlying nanoparticle (NP)-induced toxicity in marine bivalves are not fully understood, their chemical reactivity and surface properties can promote the generation of reactive oxygen species (ROS), leading to oxidative stress and activation of antioxidant defenses [12,19].

The antioxidant responses of *R. decussatus* varied consistently with Cu form, tissue, and exposure matrix, revealing distinct patterns between CuO NPs and ionic Cu (Figure 3). Superoxide dismutase (SOD), a cytosolic Cu/Zn-containing enzyme, represents the first line of defense by catalyzing the conversion of superoxide radicals ($O_2\bullet^-$) into hydrogen peroxide (H_2O_2) and Cu/Zn-SOD was identified in *Mytilus edulis* and *R. decussatus* [43,44].

SOD activity was stable in control clams ($p > 0.05$). Under exposure, clear differences between Cu forms were observed in both tissues. CuO NPs induced a progressive increase in SOD activity, particularly in the digestive gland, where values rose significantly over time in both experimental systems (4-fold and 2-fold, respectively) (Figure 3C,D; $p < 0.05$). This pattern suggests sustained superoxide production and activation of primary antioxidant defenses and likely reflects CuO NP accumulation patterns (Figure 2). In contrast, ionic Cu produced more variable responses, with significant increases mainly in the gills under water/sediment conditions (2-fold, Figure 3B), while the digestive gland showed either no significant changes in the water system (Figure 3C) or transient increases in the water/sediment system (Figure 3D). This indicates that CuO NPs elicit a more persistent oxidative challenge, whereas ionic Cu responses are more strongly influenced by environmental conditions and bioavailability.

These results are consistent with findings in other bivalves, including *M. galloprovincialis* and the freshwater species *C. rubens*, where SOD activity generally increased following CuO NP exposure [40,41,45] and similar increases in SOD activity have been reported in *M. galloprovincialis* gills exposed to Cu-based NPs, including coating-dependent effects [39] while in the digestive gland SOD activity increased after 7 days and then declined, suggesting reduced superoxide production [12]. In contrast, Geret et al. [43] reported a rapid, concentration-dependent increase in SOD activity in *R. decussatus* following ionic Cu exposure.

Catalase (CAT), a peroxisomal enzyme which detoxifies hydrogen peroxide (H_2O_2) into water and oxygen [46], showed a complementary pattern to SOD. Under CuO NP exposure, CAT activity increased significantly in both tissues (up to 3-fold; $p < 0.05$), particularly in the water system, reflecting sustained H_2O_2 production and the activation of downstream antioxidant defenses (Figure 3E,G). Conversely, ionic Cu exposure generally resulted in unchanged or decreased CAT activity, especially in the gills, in both systems possibly due to enzyme consumption in Fenton-type reactions or inhibition of enzymatic activity (Figure 3E,F). In the water/sediment system, CAT responses were attenuated for both Cu forms, reinforcing the role of the matrix in modulating Cu reactivity (Figure 3F,H).

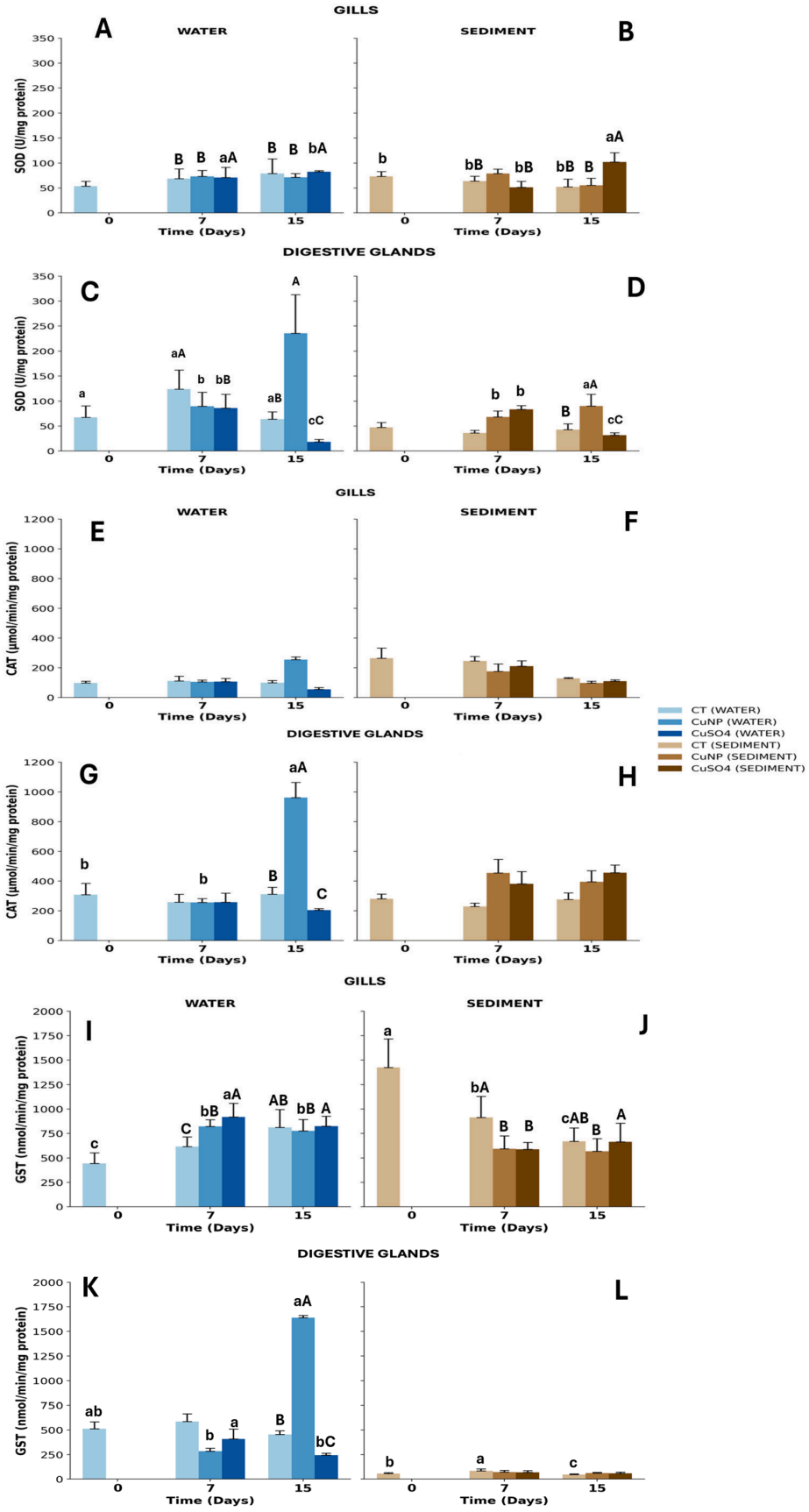

Figure 3. SOD (**A**–**D**), CAT (**E**–**H**) and GST (**I**–**L**) activities in gills and digestive gland of *R. decussatus* unexposed and exposed to CuO NPs and Cu^{2+} for 15 days in water and in a water/sediment matrix. Capital letters represent differences between treatments at the same time of exposure and lower letters differences between time of exposure ($p < 0.05$).

The increase in CAT activity in both tissues under CuO NP exposure, particularly in the water system, likely reflects enhanced ROS production, especially H_2O_2, highlighting the important role of CAT in ROS detoxification. Similar responses have been reported in *M. galloprovincialis* exposed to Cu–ZnO NPs [45]. Conversely, reduced CAT activity has been observed in *R. philippinarum* exposed to Cu associated with graphene NPs, and an inhibitory effect on CAT activity has also been reported in clams exposed to ionic Cu alone and in *R. philippinarum* after short-term exposure [47].

Taken together, these results indicate that CuO NPs elicit a more robust and coordinated antioxidant response—characterized by sustained SOD induction and elevated CAT activity—consistent with prolonged ROS generation. In contrast, ionic Cu induces weaker, less consistent, and more environmentally modulated responses, suggesting differences in uptake pathways, intracellular processing, and redox behavior between Cu forms.

The antioxidant system operates as a coordinated cascade involving SOD, CAT, and GST to mitigate ROS generated by Cu exposure. Following SOD-mediated conversion of superoxide radicals into hydrogen peroxide and its subsequent detoxification by CAT, glutathione S-transferases (GSTs) provide another defense line by conjugating glutathione (GSH) to endogenous and xenobiotic compounds, including lipid peroxidation by-products, thereby facilitating their detoxification and excretion. GSTs are widely used as biomarkers of cellular defense and oxidative stress susceptibility [48,49].

In control clams, GST activity in both gills and digestive gland showed temporal variations ($p < 0.05$; Figure 3I–L), but without exposure-related trends. Under Cu exposure, GST responses mirrored and complemented the SOD–CAT patterns, particularly in the digestive gland. In the water system, CuO NP exposure induced a marked increase in GST activity (up to 4-fold; Figure 3K); $p < 0.05$), consistent with the strong SOD and CAT induction observed in this condition, indicating enhanced ROS pressure and increased detoxification demand. In contrast, ionic Cu produced a decrease in GST activity in the digestive gland (approximately 2-fold; Figure 3K; $p < 0.05$), aligning with the weaker or more transient SOD and CAT responses, suggesting a lower or more efficiently controlled oxidative challenge.

In the gills, GST activity showed a similar but less pronounced pattern (Figure 3I), with an initial increase after 7 days followed by inhibition toward the end of exposure, paralleling the transient SOD activation observed under ionic Cu and the more sustained response under CuO NPs. In the water/sediment system, GST activity was generally attenuated for both Cu forms (Figure 3J), consistent with the reduced SOD and CAT responses and indicating lower bioavailability and oxidative stress in the presence of sediments.

An increase in GST activity suggests enhanced utilization of GSH in conjugation reactions in the digestive gland, likely linked to the formation of lipid hydroperoxides resulting from membrane lipid peroxidation induced by CuO NP exposure. A relationship between NP exposure and GST induction has previously been reported in the clam *Scrobicularia plana* exposed to CuO NPs (10 μg L^{-1}, 40–500 nm) [50]. Similarly, GST activation was observed in *R. philippinarum* exposed to graphene NPs with added Cu and to ionic Cu [47]. In the gills and digestive gland of the freshwater mussel *C. rubens*, GST activity and GSH levels also increased following CuO NP exposure [41]. Moreover, proteomic analyses using the same type of CuO NPs showed that GST was overexpressed in the gills and digestive gland of *M. galloprovincialis* [51].

Nevertheless, it is noteworthy that the observed oxidative stress cascade did not translate into significant alterations in the total protein content of the analyzed tissues. The results showed that total protein levels in both gills and digestive glands remained stable throughout the experimental period ($p > 0.05$), regardless of the exposure matrix (water or water/sediment) or the copper form (ionic or nanoparticulate) ($p > 0.05$). This stability is

crucial, as it validates the use of total protein as a robust normalization factor for enzymatic activities (e.g., SOD, CAT) and other biochemical markers in this species. By ensuring that the denominator in specific activity calculations remained unaffected by the treatments, the observed fluctuations in biomarker responses reflect genuine physiological changes in the antioxidant defense system, rather than artifacts of tissue degradation or biomass loss.

Overall, GST responses reinforce the SOD–CAT findings, confirming that CuO NPs elicit a stronger and more sustained oxidative stress cascade, whereas ionic Cu induces weaker and more matrix-dependent antioxidant activation.

3.5. Metallothioneins (MTs)

Bivalve molluscs employ several strategies to cope with excess metals, including the induction of metallothioneins (MTs) [28]. MTs are low-molecular-weight, cysteine-rich proteins induced by metals such as Cu, playing a central role in detoxification and in the regulation of metal-induced oxidative stress [52]. In cells exposed to ionic Cu, MTs bind excess Cu ions, thereby contributing to intracellular metal homeostasis and limiting the availability of redox-active Cu that can fuel ROS production.

In the present study, MT responses followed the oxidative stress cascade observed for SOD, CAT, and GST, reflecting their role in downstream detoxification (Figure 4A–D). MT levels in control clams remained stable over time in both tissues ($p > 0.05$; Figure 4A–D). In the gills, CuO NP exposure induced a slight but sustained increase in MT levels in the water-only system, particularly after 7 days, with consistently higher values than in the water/sediment system (Figure 4A,B). This pattern is consistent with the stronger SOD and CAT induction observed under the same conditions, suggesting that enhanced ROS production and Cu availability triggered both antioxidant activation and metal-binding detoxification pathways.

In clams exposed to ionic Cu, gills MT levels showed a similar but not significantly different pattern between Cu forms and matrices (Figure 4B), in agreement with the more variable SOD and CAT responses observed for this exposure condition. Comparable MT induction was reported in *R. decussatus* gills following short-term ionic Cu exposure [43], whereas in *M. galloprovincialis* a more pronounced and linear MT increase was associated with stronger oxidative and metal stress responses under CuO NP exposure [19].

In the digestive gland, MT levels showed only modest changes relative to controls ($p > 0.05$), although a slight increase was observed after 7 days under CuO NP exposure, particularly in the water-only system (Figure 4C,D). This moderate induction, compared with the stronger SOD–CAT–GST responses in the same tissue, suggests that MT-mediated sequestration contributes to Cu detoxification but may be secondary to antioxidant defenses under these exposure conditions. Lower MT levels in the water/sediment system (Figure 4D) further support a reduced metal bioavailability, consistent with the attenuated antioxidant responses observed for SOD, CAT, and GST.

Overall, MT responses complement the antioxidant cascade by contributing to Cu detoxification once ROS-scavenging systems (SOD, CAT, and GST) are activated. Together, these mechanisms indicate that CuO NPs induce a more sustained oxidative and metal stress response, requiring both enzymatic antioxidant defenses and MT-mediated sequestration, whereas ionic Cu exposure results in more variable and environmentally modulated responses. In *R. decussatus*, MTs likely contribute to Cu sequestration and elimination through Cu–MT complex formation and subsequent exocytosis [53], while additional buffering may be provided by low-molecular-weight ligands such as glutathione [42].

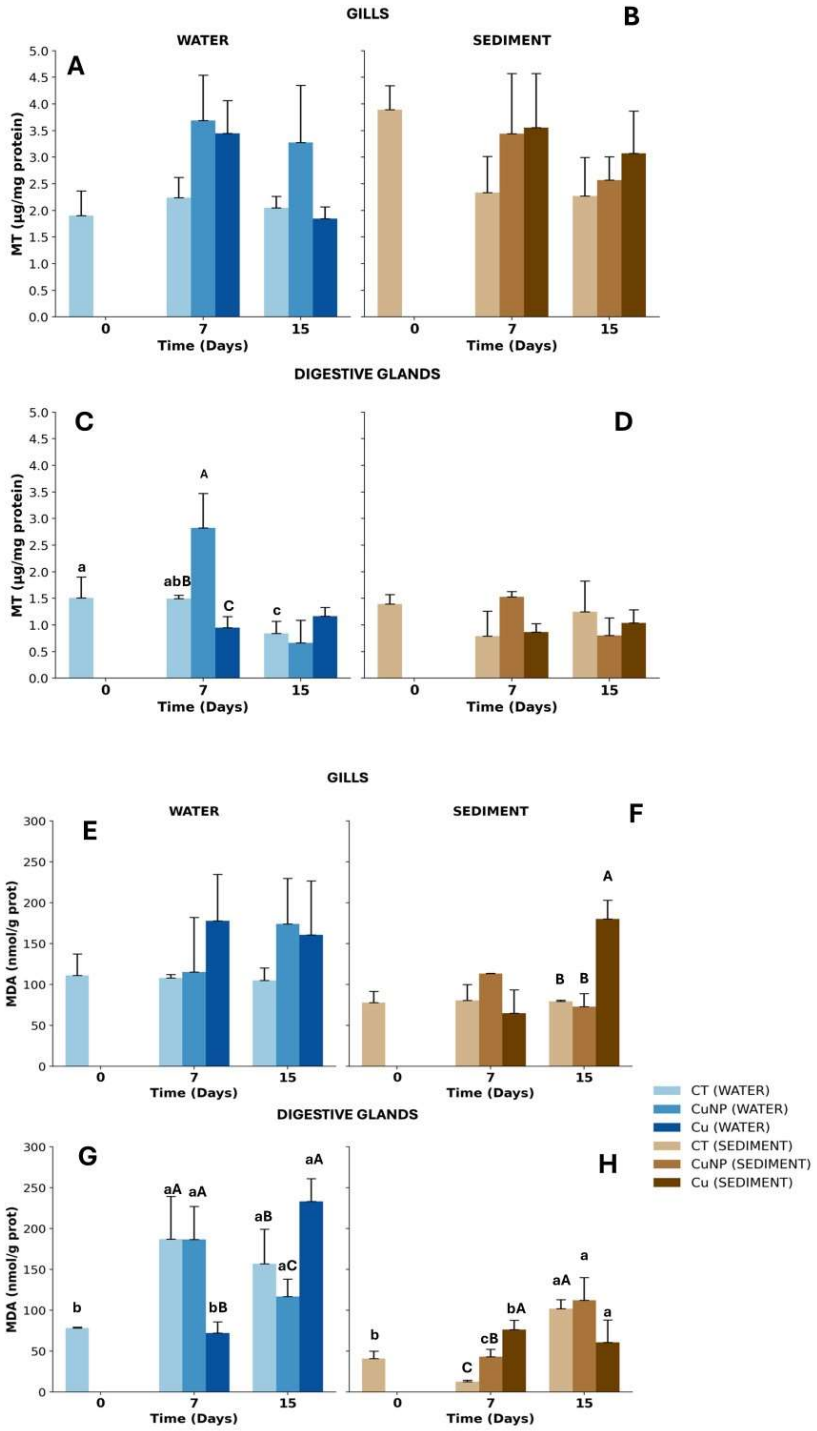

Figure 4. MTs concentrations (mg g^{-1} protein) (**A**–**D**) and lipid peroxidation (nmol g^{-1} $protein^{-1}$) (**E**–**H**) in gills and digestive gland of *R. decussatus* unexposed and exposed to CuO NPs and Cu^{2+} for 15 days a water system and in a water/sediment matrix. Capital letters represent differences between treatments at the same time of exposure and lower letters differences between time of exposure ($p < 0.05$).

3.6. Oxidative Damage

Lipid peroxidation (LPO) was used as an indicator of oxidative damage and represents a downstream consequence of ROS accumulation when antioxidant and detoxification systems are insufficient. In the water system, LPO levels in the gills increased over time under both CuO NP and ionic Cu exposure ($p < 0.05$; Figure 4E), indicating that ROS generation, despite the activation of SOD, CAT, and GST, exceeded the antioxidant and detoxification

capacity, leading to membrane damage. This effect was more pronounced under CuO NP exposure, consistent with the stronger and more sustained activation of upstream antioxidant defenses and MT induction, reflecting higher overall oxidative pressure.

In the water/sediment system, LPO responses were generally attenuated (Figure 4F,H), in line with the reduced SOD, CAT, GST, and MT responses observed under these conditions. Under CuO NP exposure, LPO increased transiently in the gills after 7 days but returned to control levels by the end of the experiment (Figure 4F), suggesting an initial oxidative challenge followed by effective compensation through antioxidant and detoxification mechanisms. In contrast, ionic Cu induced a delayed increase in LPO, indicating slower but more persistent oxidative effects, likely related to temporal changes in Cu bioavailability and uptake (Figure 4F).

In the digestive gland, LPO remained largely unchanged under CuO NP exposure (Figure 4G), despite moderate induction of antioxidant and MT responses, suggesting effective intracellular buffering of ROS and Cu through coordinated SOD–CAT–GST activity and metal sequestration. Conversely, ionic Cu exposure led to increased LPO in the water system, highlighting a tissue-specific vulnerability of the digestive gland when antioxidant defenses are less strongly or transiently activated.

Overall, LPO results confirm that oxidative damage arises when ROS production surpasses the combined capacity of antioxidant enzymes (SOD, CAT, GST) and metal-binding defenses (MTs). The strongest lipid damage occurred under CuO NP exposure in the water-only system (Figure 4E), while the presence of sediment consistently mitigated oxidative stress (Figure 4F,G), reinforcing its role in reducing Cu bioavailability and biological impact.

3.7. DNA Damage

To assess whether the two Cu forms induce genotoxicity in *R. decussatus*, the Comet assay was applied to clam hemolymph, and the results are presented in Figure 5A,B. In control clams, the percentage of DNA in the tail (% DNA tail) remained stable over time in both exposure systems ($p > 0.05$). In contrast, clams exposed to CuO NPs in both systems showed a significant time-dependent increase in % DNA tail compared with controls ($p < 0.05$; Figure 5), indicating clear genotoxic effects. This pattern is consistent with the stronger oxidative stress response observed for CuO NPs, characterized by sustained activation of SOD, CAT, GST, and MTs, and increased lipid peroxidation, suggesting that excessive ROS production contributed to DNA strand breaks. Similar responses have been reported in *M. galloprovincialis* hemocytes exposed to CuO NPs of comparable size and concentration [35] and in *Mytilus* spp. gills and hemocytes after short-term exposure, with variability depending on nanoparticle coating [39].

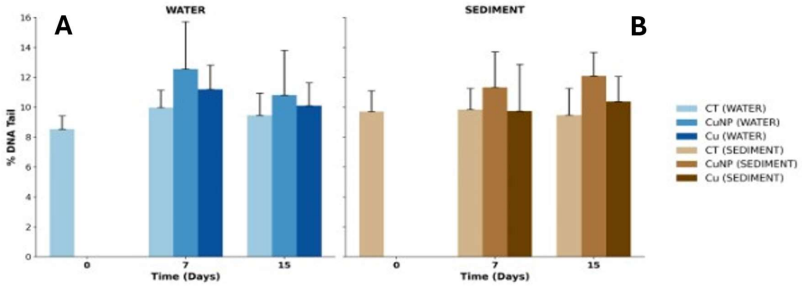

Figure 5. DNA damage (% DNA Tail) in the hemolymph of *R. decussatus* unexposed and exposed to CuO NPs and Cu^{2+} for 15 days in water (**A**) and in a water/sediment matrix (**B**).

Exposure to ionic Cu also resulted in a significant increase in DNA strand breaks after 7 days ($p < 0.05$; Figure 5A), although the effect was generally lower and more transient than that observed for CuO NPs, with values stabilizing toward the end of exposure ($p > 0.05$).

No significant differences between Cu forms were observed in the water/sediment system (Figure 5B), consistent with the overall attenuation of antioxidant and oxidative damage responses under these conditions.

The genotoxic effects of ionic Cu are most likely linked to ROS formation and consequent oxidative damage, as supported by the parallel activation of antioxidant defenses observed in this study and reported for other aquatic species [35,54]. However, the weaker and more transient DNA damage compared with CuO NPs suggests a lower or more efficiently controlled oxidative burden, in agreement with the less sustained SOD–CAT–GST responses.

For CuO NPs, DNA damage is generally attributed to oxidative DNA lesions rather than direct interaction with genetic material, arising from both particle-associated effects and Cu ion release. Once internalized, CuO NPs can promote radical formation that disrupts cellular redox balance, leading to oxidative damage to lipids, proteins, and DNA [55–57]. This mechanism is consistent with the pronounced oxidative stress cascade observed here.

Comparative studies further support this interpretation. In *R. philippinarum*, CuO NP exposure (25–55 nm) induced higher DNA strand breaks than bulk Cu but lower than ionic Cu, suggesting that genotoxicity is strongly influenced by dissolution kinetics rather than particle size alone [38]. Overall, in *R. decussatus*, the observed DNA damage following CuO NP exposure is best explained by sustained ROS production and incomplete mitigation by antioxidant and detoxification systems, rather than direct DNA interaction.

3.8. Acetylcholinesterase (AChE)

Acetylcholinesterase (AChE) regulates acetylcholine (ACh) levels in synapses, which are central to neural function in bivalves [58] and AChE activity is an indicator of neurotoxicity and is widely used as a biomarker of neurotoxic effects. AChE activity in clam gills exposed to CuO NPs under both treatments is shown in Figure 6.

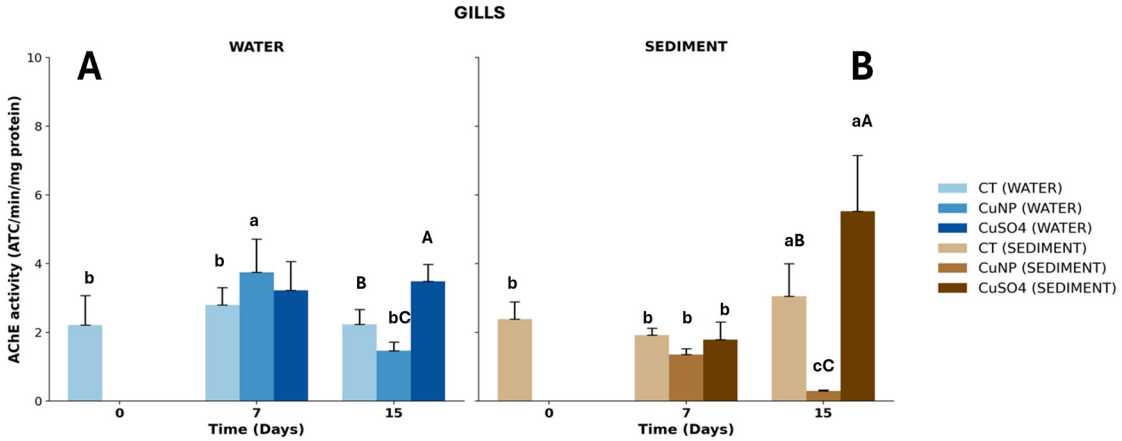

Figure 6. AChE activity in the gills of *R. decussatus* unexposed and exposed to CuO NPs and Cu^{2+} for 15 days in water (**A**) and in a water/sediment matrix (**B**). Capital letters represent differences between treatments at the same time of exposure and lower letters differences between time of exposure ($p < 0.05$).

In unexposed clams, AChE activity increased only in individuals maintained in the water/sediment system at the end of the exposure period, although the increase was not significant ($p > 0.05$; Figure 6B).

In clams exposed to CuO NPs, AChE activity showed different patterns depending on the treatment. In the water system, AChE activity increased after 7 days of exposure but significantly decreased after two weeks ($p < 0.05$: Figure 6A). This suggests that AChE

activation can represent an early warning signal or transient adaptive response before toxic damage leads to enzyme inhibition. In the water/sediment system (Figure 6B), AChE activity was initially higher and then decreased linearly over time (AChE = 2.36 − 0.14 t; $r = 0.999$), indicating neurotoxic effects associated with CuO NP exposure. A similar response was observed in the gills and digestive gland of the mussel *M. galloprovincialis* exposed to Cu–ZnO NPs [45].

AChE catalyzes the hydrolysis of ACh in the central nervous system [59], and its inhibition can lead to neuronal damage. The inhibition observed in clam gills may result from ROS production, particularly H_2O_2, induced by NP exposure, which can alter the active site of AChE [60], or from inflammatory processes. Additionally, Cu released from CuO NPs may inhibit cholinesterase (ChE) by forming complexes with sulfhydryl groups of the enzyme, disrupting its normal function and affecting the nervous system.

In contrast, AChE activity in clam gills exposed to dissolved Cu remained unchanged in the water system (Figure 6A), while in the water/sediment system, AChE activity significantly increased 1.8-fold by the end of the experiment ($p < 0.05$; Figure 6B), indicating that the increase in AChE activity observed in bivalves may reflect a compensatory response aimed at maintaining cholinergic neurotransmission under stress conditions. AChE plays a key role in regulating acetylcholine levels and is involved not only in neural function but also in neuroimmune interactions, which can be activated by environmental stressors. Transient increases in AChE activity following exposure to contaminants or abiotic stress, often precede inhibitory effects, suggesting an early adaptive response of the organism. Similarly, Cazenave et al. [61] reported an approximately 1.8-fold increase in AChE activity in the invasive freshwater bivalve *L. fortunei* after exposure to Cu (50 and 200 µg Cu L^{-1}) at 15 °C, suggesting cumulative negative effects of both factors.

Conversely, AChE activity in *M. galloprovincialis* gills was inhibited after exposure to Cu (10 µg L^{-1} for 15 days) in both nano (CuO NPs) and ionic forms [35]. In *M. edulis* gills, changes in AChE activity were concentration dependent, with higher Cu levels (200 µg L^{-1}) inhibiting the enzyme, whereas lower concentrations showed time-dependent effects [62]. Differences in AChE responses to Cu exposure may also be related to MTs induction in this species, which plays a role in Cu homeostasis and detoxification [42] The mussel *M. galloprovincialis* seems to be sensitive to Cu–ZnO NPs, and the inhibition of AChE may result from the strong binding affinity of Cu to the thiol residues of AChE [45], as also observed in the present case for binding to the sulfur residues of MTs.

Interestingly, the pattern of AChE activity is similar to that observed for LPO levels. Some studies in other animal models have reported AChE activation alongside increased LPO [61] (Cazenave et al., 2025). In this case, the effect of metals on AChE activity may be due to disruption of the plasma membrane caused by increased lipid peroxidation [63]. Furthermore, AChE may be associated with cell apoptosis and subsequent release of the enzyme, as reported by Zhang and Shi (2002) [64]. In *M. galloprovincialis*, exposure to CuO induced antioxidant effects mainly related to GST, apoptosis, and proteolysis; however, this needs to be confirmed in *R. decussatus* [51].

3.9. Comparison Between Water and Water/Sediment System

To compare the effects of nano and ionic Cu in water and water/sediment systems, a PCA was performed (Figure 7). The analysis clearly separates Cu-exposed samples from controls along PC1, while PC2 distinguishes tissue-specific responses (gills vs. digestive gland) driven by exposure type and duration. Overall, PCA highlights oxidative stress and neurotoxicity, particularly in gill tissues. Gill-related biomarkers (LPO, SOD, and AChE) are strongly associated with the positive end of PC1, especially under ionic Cu exposure in sediments after 15 days and under both Cu forms in water after 7 days. This indicates

pronounced oxidative stress and potential neurotoxicity in gills under these conditions. The close alignment of SOD and LPO vectors suggests a strong positive correlation, indicating that antioxidant defenses are insufficient to prevent membrane damage. Similarly, MT in the digestive gland and GST in the gills show parallel trends, suggesting coordinated responses to stress.

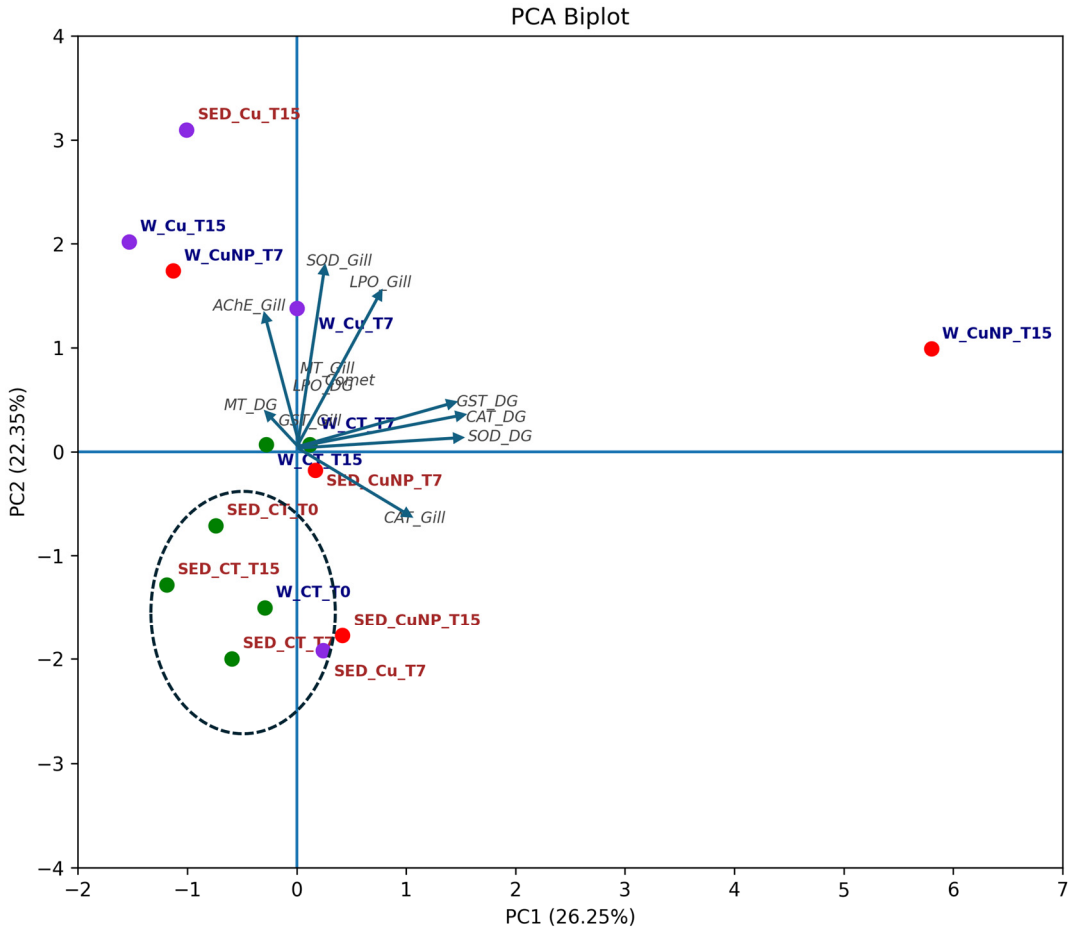

Figure 7. PCA of a battery of biomarkers measured in the gills of *R. decussatus* unexposed (CT) and exposed to CuO NPs and Cu^{2+} for 15 days in water (W) and in a water/sediment matrix (SED).

The Comet assay vector aligns with the positive axis of PC1, indicating that DNA damage is a central biological response to both exposure types in the water system and is closely associated with systemic oxidative stress across tissues. Accordingly, DNA damage represents a key component of the toxicological profile of organisms exposed to both types of copper in the waterborne system and to ionic Cu in water/sediment system at the end of the exposure period.

Control groups and short-term exposures clustered near the negative side of PC1, indicating minimal biological effects. Overall, water/sediment exposure ranged from negligible effects to pronounced gill stress under prolonged ionic Cu exposure, whereas waterborne CuO NPs progressively targeted the digestive gland. Thus, ionic and nanoparticulate Cu exhibit distinct, tissue-specific, and time-dependent toxicological profiles.

Exposure duration influenced response patterns. CuO NP exposure shifted from gill-dominated responses at 7 days to stronger digestive gland involvement at 15 days. In the water system, CuO NPs were increasingly associated with digestive gland biomarkers (SOD, CAT, GST) (Figure 3), highlighting this tissue's central role in nanoparticle detoxification. In contrast, under water/sediment conditions, nanoparticle exposure produced a profile similar to controls, indicating lower physiological impact. This might indicate that the CuO

NPs that have reached the sediments were either in small amounts either in the particulate form or dissolved.

Ionic Cu showed a different pattern. After 7 days in the water system, responses were mainly associated with gill stress and metallothionein (MT), with a weaker shift toward digestive gland involvement than observed for nanoparticles. Prolonged exposure in the water/sediment system resulted in the highest overall stress, strongly linked to gill responses, including oxidative damage and neurotoxicity.

The observed cytotoxic, genotoxic, and oxidative stress responses, together with potential bioaccumulation, highlight the environmental relevance of CuO NPs in marine bivalves [39]. Similar effects—including oxidative stress, MT induction, and AChE inhibition—have been reported in *M. galloprovincialis* exposed to ionic Cu (10 μg L^{-1}) [12,19].

Both Cu forms induced oxidative stress in *R. decussatus* (Figure 7), but with distinct patterns: ionic Cu was mainly associated with genotoxicity and early digestive gland damage, whereas CuO NPs caused acute gill stress followed by a strong enzymatic response in the digestive gland.

Multivariate analysis highlights the exposure medium as a key driver of toxicity, directing Cu toward different physiological compartments. In water-only systems, ionic Cu triggered early genotoxicity and oxidative stress in the gills, preceding full activation of enzymatic defenses. In contrast, nanoparticles increasingly affected the digestive gland over time, requiring enhanced antioxidant and detoxification responses (SOD, GST).

In the water/sediment system, ionic Cu caused the most pronounced effects, with severe oxidative damage and neurotoxicity in the gills. Conversely, CuO NPs clustered with controls, suggesting reduced bioavailability. This likely reflects limited dissolution of CuO NPs (~1%) in marine conditions, emphasizing the role of sediments in mitigating nanoparticle toxicity and its relevance for environmental risk assessment.

As *R. decussatus* is both economically important and ecologically relevant, these toxic effects may impair ecosystem functioning and impact on the blue economy. The shift from gill stress to longer-term digestive gland responses suggests that CuO NP pollution disrupts multiple physiological pathways, potentially reducing population resilience and altering food web dynamics. Because bivalves accumulate contaminants and are widely consumed, the observed oxidative stress and genotoxicity in *R. decussatus* indicate potential risks for trophic transfer. Although human health was not directly assessed, these mechanisms are conserved across species and are linked to disease processes.

Overall, these findings demonstrate that emerging contaminants such as CuO NPs affect multiple biological systems and share toxicity pathways (e.g., oxidative stress and genotoxicity) relevant to both wildlife and humans. They also highlight *R. decussatus* as an effective early indicator of environmental and public health risks. Notably, waterborne nanoparticle exposure may pose greater risks than sediment-bound forms for this species, with implications for monitoring and regulation. CuO NPs induce pronounced biochemical and cellular stress, including DNA damage and impaired antioxidant defenses. In a One Health context, bivalves act as sentinel species, reflecting environmental health. Biomarkers such as SOD, LPO, AChE, and DNA damage provide early warning signals of CuO NP contamination that may also affect other marine organisms, including commercially important species.

These results underscore the need for integrated risk assessment strategies that consider environmental exposure, ecological effects, and human health together. A One Health approach strengthens the case for regulating nanoparticle emissions and incorporating biomarker-based monitoring into coastal management programs.

4. Conclusions

Both CuO NPs and ionic Cu pose significant risks to marine organisms, inducing oxidative stress, oxidative damage, genotoxicity, and biochemical disruption in *R. decussatus*. However, toxicity depends on Cu form and exposure route, highlighting the importance of understanding accumulation dynamics for accurate environmental risk assessment and mitigation.

CuO nanoparticles elicit faster and stronger stress responses than ionic Cu under waterborne exposure, particularly at early stages, indicating higher acute toxicity. Ionic Cu is primarily associated with early genotoxicity and oxidative damage, whereas CuO NPs drive a shift from initial gill stress to digestive gland-mediated detoxification over time.

Waterborne exposure to both CuO NPs and ionic Cu affects different biological pathways than sediment-bound Cu, emphasizing the role of exposure route and duration in shaping toxicological outcomes.

The combined evidence of oxidative stress, genotoxicity, and potential bioaccumulation in *R. decussatus* suggests that CuO NPs represent an emerging environmental risk to marine ecosystems.

Overall, these findings highlight the need for integrated One Health approaches to assess ecological and potential human health risks associated with nanoparticle pollution.

Supplementary Materials: The following supporting information can be downloaded at: https://www.mdpi.com/article/10.3390/fishes11050282/s1, Table S1: Summary of Two-way ANOVA results for biochemical biomarkers in *R. decussatus*. The analysis considers the main effects of Treatment (Control, Cu-ionic, and CuO-NPs), Exposure Time (0, 7 and 15 days), and their Interaction, for both tissues (gills and digestive glands) and exposure matrices (water and sediment).

Author Contributions: Conceptualization, M.J.B.; methodology, M.T., T.L.R. and T.G. (Tânia Gomes); validation, M.J.B.; formal analysis, M.T. and T.G. (Taina Garcia); investigation, T.L.R. and T.G. (Taina Garcia); resources, M.J.B.; data curation, T.L.R. and T.G. (Taina Garcia); writing—original draft, M.J.B.; supervision, T.G. (Tânia Gomes) and T.G. (Taina Garcia). All authors have read and agreed to the published version of the manuscript.

Funding: The authors acknowledge the funding provided by FCT for projects LA/P/0069/2020, awarded to the Associate Laboratory ARNET (https://doi.org/10.54499/LA/P/0069/2020) and UID/00350/2020 (https://doi.org/10.54499/UID/00350/2025), awarded to CIMA of the University of the Algarve.

Institutional Review Board Statement: Ethical approval is not required in Portugal for work on bivalves.

Informed Consent Statement: Not applicable.

Data Availability Statement: The original contributions presented in this study are included in the article. Further inquiries can be directed to the corresponding authors.

Conflicts of Interest: The authors declare no conflicts of interest.

References

1. Rocha, T.L.; Gomes, T.; Sousa, V.S.; Mestre, N.C.; Bebianno, M.J. Ecotoxicological impact of engineered nanomaterials in bivalve molluscs: An overview. *Mar. Environ. Res.* **2015**, *111*, 74–88. [CrossRef]
2. Sleeman, J.M.; DeLiberto, T.; Nguyen, N. Optimization of human, animal, and environmental health by using the One Health approach. *J. Vet. Sci.* **2017**, *18*, 263–268. [CrossRef]
3. Destoumieux-Garzón, D.; Mavingui, P.; Boetsch, G.; Boissier, J.; Darriet, F.; Duboz, P.; Fritsch, C.; Giraudoux, P.; Le Roux, F.; Morand, S.; et al. The one health concept: 10 Years old and a long road ahead. *Front. Vet. Sci.* **2018**, *5*, 14. [CrossRef]
4. Baker, T.J.; Tyler, C.R.; Galloway, T.S. Impacts of metal and metal oxide nanoparticles on marine organisms. *Environ. Pollut.* **2014**, *186*, 257–271. [CrossRef]

5. Griffitt, R.J.; Weil, R.; Hyndman, K.A.; Denslow, N.D.; Powers, K.; Taylor, D.; Barber, D.S. Exposure to copper nanoparticles causes gill injury and acute lethality in zebrafish (*Danio rerio*). *Environ. Sci. Technol.* **2007**, *41*, 8178–8186. [CrossRef]
6. Miller, R.J.; Adeleye, A.S.; Page, H.M.; Kui, L.; Lenihan, H.S.; Keller, A.A. Nano and traditional copper and zinc antifouling coatings: Metal release and impact on marine sessile invertebrate communities. *J. Nanopart. Res.* **2020**, *22*, 129. [CrossRef]
7. Esposito, G.; Pastorino, P.; Prearo, M.; Magara, G.; Cesarani, A.; Freitas, R.; Caldaroni, B.; Meloni, D.; Pais, A.; Dondo, A.; et al. Ecotoxicity of copper(I) chloride in grooved carpet shell (*Ruditapes decussatus*). *Antioxidants* **2022**, *11*, 2148. [CrossRef]
8. Handy, R.D.; Kammer, F.; Lead, J.R.; Hassellöv, M.; Owen, R.; Crane, M. The ecotoxicology and chemistry of manufactured nanoparticles. *Ecotox* **2008**, *17*, 287–314. [CrossRef]
9. Griffitt, R.J.; Hyndman, K.; Denslow, N.D.; Barber, D.S. Comparison of molecular and histological changes in zebrafish gills exposed to metallic nanoparticles. *Toxicol. Sci.* **2009**, *107*, 404–415. [CrossRef]
10. Buffet, P.-E.; Poirier, L.; Zalouk-Vergnoux, A.; Lopes, C.; Amiard, J.-C.; Gaudin, P.; Risso-de Faverney, C.; Guibbolini, M.; Gilliland, D.; Perrein-Ettajani, H.; et al. Biochemical and behavioural responses of the marine polychaete Hediste diversicolor to cadmium sulfide quantum dots (CdS QDs): Waterborne and dietary exposure. *Chemosphere* **2014**, *100*, 63–70. [CrossRef]
11. Buffet, P.-E.; Richard, M.; Caupos, F.; Vergnoux, A.; Perrein-Ettajani, H.; Luna-Acosta, A.; Akcha, F.; Amiard, J.-C.; Amiard-Triquet, C.; Guibbolini, M.; et al. A mesocosm study of fate and effects of CuO nanoparticles on endobenthic species (*Scrobicularia plana*, *Hediste diversicolor*). *Environ. Sci. Technol.* **2013**, *47*, 1620–1628. [CrossRef]
12. Gomes, T.; Pereira, C.G.; Cardoso, C.; Pinheiro, J.P.; Cancio, I.; Bebianno, M.J. Accumulation and toxicity of copper oxide nanoparticles in the digestive gland of *Mytilus galloprovincialis*. *Aquat. Toxicol.* **2012**, *118–119*, 72–79. [CrossRef]
13. Gunawan, C.; Teoh, W.Y.; Marquis, C.P.; Amal, R. Cytotoxic origin of copper (II) oxide nanoparticles: Comparative studies with micron-sized particles, leachate, and metal salts. *ACS Nano* **2011**, *5*, 7214–7225. [CrossRef]
14. Abdel-Khalek, A.A.; Kadry, M.M.; Badran, S.R.; Marie, M.S. Comparative toxicity of copper oxide bulk and nano particles in Nile Tilapia; *Oreochromis niloticus*: Biochemical and oxidative stress. *J. Basic Appl. Zool.* **2015**, *72*, 43–57. [CrossRef]
15. Pang, C.; Selck, H.; Misra, S.K.; Berhanu, D.; Dybowska, A.; Valsami-Jones, E.; Forbes, V.E. Effects of sediment-associated copper to the deposit-feeding snail, *Potamopyrgus antipodarum*: A Comparison of Cu added in aqueous form or as nano- and micro-CuO particles. *Aquat. Toxicol.* **2012**, *106–107*, 114–122. [CrossRef]
16. Hanna, S.K.; Miller, R.J.; Muller, E.B.; Nisbet, R.M.; Lenihan, H.S. Impact of engineered zinc oxide nanoparticles on the individual performance of *Mytilus galloprovincialis*. *PLoS ONE* **2013**, *8*, e61800. [CrossRef]
17. Klaper, R.; Crago, J.; Barr, J.; Arndt, D.; Setyowati, K.; Chen, J. Toxicity biomarker expression in daphnids exposed to manufactured nanoparticles: Changes in toxicity with functionalization. *Environ. Pollut.* **2009**, *157*, 1152–1156. [CrossRef]
18. Andral, B.; Galgani, F.; Tomasino, C.; Bouchoucha, M.; Blottiere, C.; Scarpato, A.; Benedicto, J.; Deudero, S.; Calvo, M.; Cento, A. Chemical contamination baseline in the Western basin of the Mediterranean Sea based on transplanted mussels. *Arch. Environ. Contam. Toxicol.* **2011**, *61*, 261–271. [CrossRef]
19. Gomes, T.; Pinheiro, J.P.; Cancio, I.; Pereira, C.G.; Cardoso, C.; Bebianno, M.J. Effects of copper nanoparticles exposure in the mussel *Mytilus galloprovincialis*. *Environ. Sci. Technol.* **2011**, *45*, 9356–9362. [CrossRef]
20. Roma, J.; Matos, A.R.; Vinagre, C.; Duarte, B. Engineered metal nanoparticles in the marine environment: A review of the effects on marine fauna. *Mar. Environ. Res.* **2015**, *161*, 105110. [CrossRef]
21. Thit, A.; Banta, G.T.; Selck, H. Bioaccumulation, subcellular distribution and toxicity of sediment-associated copper in the ragworm *Nereis diversicolor*: The relative importance of aqueous copper, copper oxide nanoparticles and microparticles. *Environ. Pollut.* **2015**, *202*, 50–57. [CrossRef]
22. Thit, A.; Dybowska, A.; Kobler, C.; Kennaway, G.; Selck, H. Influence of copper oxide nanoparticle shape on bioaccumulation, cellular internalization and effects in the Estuarine sediment-dwelling polychaete, *Nereis diversicolor*. *Mar. Environ. Rese.* **2015**, *111*, 89–98. [CrossRef]
23. Bebianno, M.J.; Géret, F.; Hoarau, P.; Serafim, M.A.; Coelho, M.R.; Gnassia-Barelli, M.; Roméo, M. Biomarkers in *Ruditapes decussatus*: A potential biondicator species. *Biomarkers* **2004**, *9*, 305–330. [CrossRef]
24. Ohshima, H.; Kondo, T. Electrophoresis of large colloidal particles with surface charge layers. Position of the slipping plane and surface layer thickness. *Colloid Polym. Sci.* **1986**, *264*, 1080–1084. [CrossRef]
25. NanoComposix. *Nanocomposix's Guide to Dynamic Light Scattering Measurement and Analysis*, version 1.3; NanoComposix, Inc.: San Diego, CA, USA, 2012.
26. USEPA. *Methods for Measuring the Toxicity and Bioaccumulation of Sediment-Associated Contaminants with Freshwater Invertebrates*, 2nd ed.; EPA/600/R-99/064; USEPA: Duluth, MN, USA, 2000.
27. *E1706-20 2020*; Standard Test Method for Measuring the Toxicity of Sediment-Associated Contaminants with Freshwater Invertebrates. ASTM International: West Conshohocken, PA, USA, 2020.
28. Amiard, J.-C.; Amiard-Triquet, C.; Barka, S.; Pellerin, J.; Rainbow, P.S. Metallothioneins in aquatic invertebrates: Their role in metal detoxification and their use as biomarkers. *Aquat. Toxicol.* **2006**, *76*, 160–202. [CrossRef]

29. Bradford, M.M. A rapid and sensitive method for the quantitation of microgram quantities of protein utilizing the principle of protein-dye binding. *Anal. Biochem.* **1976**, *72*, 248–254. [CrossRef]
30. McCord, J.M.; Fridovich, I. Superoxide Dismutase: An enzymic function for erythrocuprein (hemocuprein). *J. Biol. Chem.* **1969**, *244*, 6049–6055. [CrossRef]
31. Greenwald, R.A. *Handbook of Methods for Oxygen Radical Research*; CRC Press: Boca Raton, FL, USA, 1985.
32. Habig, W.H.; Pabst, M.J.; Jakoby, W.B. Glutathione S-transferase: The first enzymatic step in mercapturic acid formation. *J. Biol. Chem.* **1974**, *249*, 7130–7139. [CrossRef]
33. Bebianno, M.J.; Langston, W.J. Quantification of metallothioneins in marine invertebrates using differential pulse polarography. *Port. Electrochim. Acta* **1989**, *7*, 59–64.
34. Singh, N.P.; McCoy, M.T.; Tice, R.R.; Schneider, E.L. A simple technique for quantitation of low levels of DNA damage in individual cells. *Exp. Cell. Res.* **1988**, *175*, 184–191. [CrossRef]
35. Gomes, T.; Pereira, C.G.; Cardoso, C.; Bebianno, M.J. Differential protein expression in mussels *Mytilus galloprovincialis* exposed to nano and ionic Ag. *Aquat. Toxicol.* **2013**, *136–137*, 79–90. [CrossRef]
36. Ellman, G.L.; Courtney, K.D.; Andres, V.; Featherstone, R.M. A new and rapid colorimetrie determination of acetylcholinesterase activity. *Biochem. Pharmacol.* **1961**, *7*, 88–95. [CrossRef]
37. Erdelmeier, I.; Gérard-Monnier, D.; Yadan, J.C.; Chaudière, J. Reactions of N-methyl-2-phenylindole with malondialdehyde and 4-hydroxyalkenals. Mechanistic aspects of the colorimetric assay of lipid peroxidation. *Chem. Res. Toxicol.* **1998**, *11*, 1184–1194. [CrossRef]
38. Volland, M.; Hampel, M.; Katsumiti, A.; Yeste, M.P.; Gatica, J.M.; Cajaraville, M.; Blasco, J. Synthesis methods influence characteristics, behaviour and toxicity of bare CuO NPs compared to bulk CuO and ionic Cu after in vitro exposure of *Ruditapes philippinarum* hemocytes. *Aquat. Toxicol.* **2018**, *199*, 285–295. [CrossRef]
39. Connolly, M.; Little, S.; Hartl, M.G.J.; Fernandes, M.T. Integrated testing strategy for ecotoxicity (ITS-ECO) assessment in the marine environmental compartment using *Mytilus* spp.: A case study using pristine and coated CuO and TiO_2 banomaterials. *Environ. Toxicol. Chem.* **2022**, *41*, 1390–1406. [CrossRef]
40. Canesi, L.; Ciacci, C.; Fabbri, R.; Marcomini, A.; Pojana, G.; Gallo, G. Bivalve molluscs as a unique target group for nanoparticle toxicity. *Mar. Environ. Res.* **2012**, *76*, 16–21. [CrossRef]
41. Morad, M.; Hassanein, T.F.; El-khadragy MFFehaid, A.; Habotta, O.A.; Moneim, A.A. Biochemical and histopathological effects of copper oxide nanoparticles exposure on the bivalve *Chambardia rubens* (Lamarck, 1819). *Biosci. Rep.* **2023**, *43*, BSR20222308. [CrossRef]
42. Serafim, A.; Bebianno, M.J. Metallothionein role in the kinetic model of copper accumulation and elimination in the clam *Ruditapes decussatus*. *Environ. Res.* **2009**, *109*, 390–399. [CrossRef]
43. Geret, F.; Serafim, A.; Barreira, L.; Bebianno, M.J. Response of antioxidant systems to copper in the gills of the clam *Ruditapes decussatus*. *Mar. Environ. Res.* **2002**, *54*, 413–417. [CrossRef]
44. Manduzio, H.; Monsinjon, T.; Rocher, B.; Leboulenger, F.; Galap, C. Characterization of an inducible isoform of the Cu/Zn superoxide dismutase in the blue mussel *Mytilus edulis*. *Aquat. Toxicol.* **2003**, *64*, 73–83. [CrossRef]
45. Bouzidi, I.; Ayari-Kliti, R.; Beyrem, H.; Mougin, K.; Sellami, B. The response of the Mediterranean mussel *Mytilus galloprovincialis* (Lamarck, 1819) exposed to copper-doped zinc nanoparticles. *J. Sed. Environ.* **2024**, *9*, 135–143. [CrossRef]
46. Takano, H.; Zou, Y.; Hasegawa, H.; Akazawa, H.; Nagai, T.; Komuro, I. Oxidative stress-induced signal transduction pathways in cardiac myocytes: Involvement of ROS in heart diseases. *Antiox Redox Signal* **2003**, *5*, 789–794. [CrossRef]
47. Britto, R.S.; Nascimento, J.P.; Serode, T.; Santos, A.P.; Soares, A.M.V.M.; Figueira, E.; Furtado, C.; Lima-Ventura, J.; Monserrat, J.M.; Freitas, R. The effects of co-exposure of graphene oxide and copper under different pH conditions in Manila clam *Ruditapes philippinarum*. *Environ. Sci. Pollut. Res.* **2020**, *27*, 30945–30956. [CrossRef]
48. McDonagh, B.; Sheehan, D. Redox proteomics in the blue mussel *Mytilus edulis*: Carbonylation is not a pre–requisite for ubiquitination in acute freeradical–mediated oxidative stress. *Aquat. Toxicol.* **2006**, *79*, 325–333. [CrossRef]
49. Ferreira, J.L.R.; Lonné, M.N.; França, T.A.; Maximilla, N.R.; Lugokenski, T.H.; Costa, P.G.; Fillmann, G.; Soares, F.A.A.; de la Torre, F.R.; Monserrat, J.M. Co-exposure of the organic nanomaterial fullerene C60 with benzo[a]pyrene in *Danio rerio* (zebrafish) hepatocytes: Evidence of toxicological interactions. *Aquat. Toxicol.* **2014**, *147*, 76–83. [CrossRef]
50. Buffet, P.-E.; Tankoua, O.F.; Pan, J.-F.; Berhanu, D.; Herrenknecht, C.; Poirier, L.; Amiard-Triquet, C.; Amiard, J.-C.; Bérard, J.-B.; Risso, C.; et al. Behavioural and biochemical responses of two marine invertebrates Scrobicularia plana and *Hediste diversicolor* to copper oxide nanoparticles. *Chemosphere* **2011**, *84*, 166–174. [CrossRef]
51. Gomes, T.; Chora, S.; Pereira, C.G.; Cardoso, C.; Bebianno, M.J. Proteomic response of mussels *Mytilus galloprovincialis* exposed to CuO NPs and Cu^{2+}: An exploratory biomarker discovery. *Aquat. Toxicol.* **2014**, *155*, 327–336. [CrossRef]
52. Langston, W.J.; Bebianno, M.J.; Burt, G.R. Metal handling strategies in molluscs. In *Metal Metabolism in the Aquatic Environment*; Langston, W.J., Bebiano, M.J., Eds.; Chapman and Hall: London, UK, 1998; pp. 219–284.

53. Viarengo, A.; Canesi, L.; Pertica, M.; Poli, G.; Moore, M.N.; Orunesu, M. Heavy metal effects on lipid peroxidation in the tissues of *Mytilus galloprovincialis* Lam. *Comp. Biochem. Physiol. Part C* **1990**, *97*, 37–42. [CrossRef]
54. Al-Subiai, S.N.; Moody, A.J.; Mustafa, S.A.; Jha, A.N. A multiple biomarker approach to investigate the effects of copper on the marine bivalve mollusc, *Mytilus edulis*. *Ecotoxicol. Environ. Saf.* **2011**, *74*, 1913–1920. [CrossRef]
55. Ahamed, M.; Siddiqui, M.; Akhtar, M.J.; Ahmad, I.; Pant, A.B.; Alhadlaq, H.A. Genotoxic potential of copper oxide nanoparticles in human lung epithelial cells. *Biochem. Biophys. Res. Commun.* **2010**, *396*, 578–583. [CrossRef]
56. Karlsson, H.L.; Cronholm, P.; Gustafsson, J.; Möller, L. Copper oxide nanoparticles are highly toxic: A comparison between metal oxide nanoparticles and carbon nanotubes. *Chem. Res. Toxicol.* **2008**, *21*, 1726–1732. [CrossRef]
57. Midander, K.; Cronholm, P.; Karlsson, H.L.; Elihn, K.; Möller, L.; Leygraf, C.; Wallinder, I.O. Surface characteristics, copper release, and toxicity of nano- and micrometer-sized copper and copper(II) oxide particles: A crossdisciplinary study. *Small* **2009**, *5*, 389–399. [CrossRef]
58. Matozzo, V.; Tomei, A.; Marin, M.G. Acetylcholinesterase as a biomarker of exposure to neurotoxic compounds in the clam Tapes philippinarum from the Lagoon of Venice. *Mar. Pollut. Bull.* **2005**, *50*, 1686–1693. [CrossRef]
59. He, S.B.; Wu, G.W.; Deng, H.H.; Liu, A.L.; Lin, X.H.; Xia, X.H.; Chen, W. Choline and acetylcholine detection based on peroxidase-like activity and protein antifouling property of platinum nanoparticles in bovine serum albumin scaffold. *Biosens. Bioelectron.* **2014**, *62*, 331–336. [CrossRef]
60. Schallreuter, K.U.; Gibbons, N.C.; Elwary, S.M.; Parkin, S.M.; Wood, J.M. Calcium-activated butyrylcholinesterase in human skin protects acetylcholinesterase against suicide inhibition by neurotoxic organophosphates. *Biochem. Biophys. Res. Commun.* **2007**, *355*, 1069–1074. [CrossRef]
61. Cazenave, J.; Rossi, A.S.; Ale, A.; Montalto, L.; Gutierrez, M.F.; Molina, F.R. Does temperature influence biomarker responses to copper exposure? The invasive bivalve *Limnoperna fortunei* (Dunker 1857) as a model. *Comp. Biochem. Physiol. C* **2025**, *287*, 110059. [CrossRef]
62. Lehtonen, K.K.; Leiniö, S. Effects of exposure to copper and malathion on metallothionein levels and acetylcholinesterase activity of the mussel *Mytilus edulis* and the clam *Macoma balthica* from the Northern Baltic Sea. *Bull. Environ. Contam. Toxicol.* **2003**, *71*, 489–496. [CrossRef]
63. Kaizer, R.R.; Corrêa, M.C.; Spanevello, R.M.; Morsch, V.M.; Mazzanti, C.M.; Gonçalves, J.F.; Schetinger, M.R.C. Acetylcholinesterase activation and enhanced lipid peroxidation after long-term exposure to low levels of aluminum on different mouse brain regions. *J. Inorg. Biochem.* **2005**, *99*, 1865–1870. [CrossRef]
64. Zhang, L.Y.; Shi, Y.F. Induction of acetylcholinesterase expression during apoptosis in various cell types. *Cell Death Differ.* **2002**, *9*, 790–800. [CrossRef]